
Article:
Horn, F.C., Marshall, H., Collier, G.J. et al. (5 more authors) (2017) Regional ventilation changes in the lung: Treatment response mapping by using hyperpolarized gas MR imaging as a quantitative biomarker. Radiology, 284 (3). pp. 854-861. ISSN 0033-8419

https://doi.org/10.1148/radiol.2017160532

Radiology

Regional Ventilation Changes in the Lung: Treatment Response Mapping by Using Hyperpolarized Gas MR Imaging as a Quantitative Biomarker[1]

Felix C. Horn, PhD
Helen Marshall, PhD
Guilhem J. Collier, PhD
Richard Kay, PhD
Salman Siddiqui, PhD
Christopher E. Brightling, PhD
Juan Parra-Robles, PhD
Jim M. Wild, PhD

Purpose: To assess the magnitude of regional response to respiratory therapeutic agents in the lungs by using treatment response mapping (TRM) with hyperpolarized gas magnetic resonance (MR) imaging. TRM was used to quantify regional physiologic response in adults with asthma who underwent a bronchodilator challenge.

Materials and Methods: This study was approved by the national research ethics committee and was performed with informed consent. Imaging was performed in 20 adult patients with asthma by using hyperpolarized helium 3 (^{3}He) ventilation MR imaging. Two sets of baseline images were acquired before inhalation of a bronchodilating agent (salbutamol 400 μg), and one set was acquired after. All images were registered for voxelwise comparison. Regional treatment response, $\Delta R(r)$, was calculated as the difference in regional gas distribution ($R[r]$ = ratio of inhaled gas to total volume of a voxel when normalized for lung inflation volume) before and after intervention. A voxelwise activation threshold from the variability of the baseline images was applied to $\Delta R(r)$ maps. The summed global treatment response map (ΔR_{net}) was then used as a global lung index for comparison with metrics of bronchodilator response measured by using spirometry and the global imaging metric percentage ventilated volume (%VV).

Results: ΔR_{net} showed significant correlation ($P < .01$) with changes in forced expiratory volume in 1 second ($r = 0.70$), forced vital capacity ($r = 0.84$), and %VV ($r = 0.56$). A significant ($P < .01$) positive treatment effect was detected with all metrics; however, ΔR_{net} showed a lower intersubject coefficient of variation (64%) than all of the other tests (coefficient of variation, ≥99%).

Conclusion: TRM provides regional quantitative information on changes in inhaled gas ventilation in response to therapy. This method could be used as a sensitive regional outcome metric for novel respiratory interventions.

Online supplemental material is available for this article.

[1] From the Unit of Academic Radiology, Department of Infection, Immunity and Cardiovascular Disease, C Floor, Royal Hallamshire Hospital, University of Sheffield, Glossop Rd, Sheffield S10 2JF, England (F.C.H., H.M., G.J.C., J.P., J.M.W.); Novartis, Basel, Switzerland (R.K.); Department of Respiratory Medicine, Glenfield Hospital, Leicester, England (S.S., C.E.B.); Insigneo Institute of In-Silico Medicine, University of Sheffield, Sheffield, England (J.M.W.).
Received March 3, 2016; revision requested April 18; revision received October 18; accepted November 28; final version accepted January 27, 2017. This article presents independent research funded by the National Institute for Health Research (NIHR). The views expressed are those of the authors and not necessarily those of the National Health Service, the NIHR, or the Department of Health.
Address correspondence to J.M.W. (e-mail: *j.m.wild@sheffield.ac.uk*).

Funding for this study was received from Novartis International, the Airway Disease Predicting Outcomes through Patient Specific Computational Modelling Network, the Pulmonary Imaging Network, and the National Institute for Health Research.

Lung function tests such as spirometry are widely used to clinically assess airflow obstruction and its reversibility, and indexes such as forced expiratory volume in 1 second (FEV_1) are commonly accepted outcome measures in the assessment of therapies for obstructive lung disease. These techniques, while established in respiratory medicine, assess the lungs as one unit, with limited sensitivity to regional ventilation changes (1). Imaging as a diagnostic tool can provide regional insight into alterations of both the structure and the function of the lungs and is increasingly being used as an outcome measure in the early-phase evaluation of respiratory therapeutic agents (2). In particular, regionally specific therapies, such as bronchial thermoplasty in asthma (3), endobronchial valve therapy (4), and lung volume reduction surgery in chronic obstructive pulmonary disease (5), require that regional information be obtained so that the efficacy of the intervention can be assessed. Previous studies have used computed tomography (CT)- and computational fluid dynamics–derived markers of airflow to assess functional changes after bronchodilator therapy (6). However, those methods rely solely on models of ventilation inferred from structural CT images acquired at different levels of inspiration and the repeated use of ionizing radiation, which could be detrimental, particularly in pediatric cohorts.

Functional lung imaging with hyperpolarized gas magnetic resonance (MR) imaging provides three-dimensional (3D) images of lung ventilation in a short breath hold. Hyperpolarized helium 3 (^{3}He) MR imaging has been shown to be a sensitive measure of ventilation heterogeneity in asthma (7,8). Although numerous metrics have been derived to describe ventilation heterogeneity from both hyperpolarized xenon 129 (^{129}Xe) and ^{3}He images by using texture-based methods like feature analysis or clustering methods such as k-means clustering (9–12), efforts have been focused on cross-sectional assessment of cohorts. Longitudinal studies and therapy assessment have focused on global outcome measures from hyperpolarized ^{3}He imaging, in particular percentage ventilated volume (%VV) or its counterpart, percentage defect volume (7,13). Although %VV has been shown to correlate with spirometric findings in asthma (14,15), the method is limited by the binary classification of ventilated versus nonventilated lung regions, sacrificing much of the richness of the regional information on lung ventilation heterogeneity present in the images. There is therefore a need for imaging metrics that fully explore the regional sensitivity of these high-resolution images of lung function to assess the success of intervention.

In this study, treatment response mapping (TRM) is introduced as a novel technique to provide regional quantitative information on changes in lung ventilation in response to therapy and is demonstrated in an asthma cohort by measuring bronchodilator response.

Advances in Knowledge

- Treatment response mapping (TRM) is a novel technique for quantitative assessment of regional lung ventilation changes in response to treatment.
- The net treatment response map integrated over the whole lungs (ΔR_{net}) correlates with changes in spirometry (Pearson correlation: $r = 0.70$ for change in forced expiratory volume in 1 second; $r = 0.84$ for change in forced vital capacity; $P < .01$).
- Compared with standard clinical outcome measures based on lung function, TRM adds information about the size and direction of the regional physiologic response of the lungs.

Implications for Patient Care

- TRM has potential for the assessment of regional lung interventions such as anti-inflammatory therapies or targeted therapies such as thermoplasty, endobronchial valve therapy, and lung volume reduction surgery.
- Potential clinical applications for TRM are pediatric and longitudinal studies of lung disease progression because patients are not exposed to ionizing radiation.

Materials and Methods

The study was approved by the national research ethics committee, and written patient consent was obtained. All data were acquired between February 2012 and June 2013, and the study was funded in parts by Novartis. One author (R.K.) was an employee of Novartis. The authors not employed by Novartis had full control of the data and of the information submitted for publication.

Study Population and Design

Twenty patients (10 women, 10 men) with a diagnosis of moderate-to-severe asthma (Global Initiative for Asthma step 2–5 [16]) were examined in this retrospective analysis. Patient age range was 21–73 years. Patients were tested for response to a bronchodilator (400 μg salbutamol) with hyperpolarized gas ventilation MR imaging and with spirometry. Patient demographic data and results of pulmonary function tests are shown in Table 1.

https://doi.org/10.1148/radiol.2017160532

Content codes: CH MR

Radiology 2017; 284:854–861

Abbreviations:
FEV_1 = forced expiratory volume in 1 second
FVC = forced vital capacity
%VV = percentage ventilated volume
3D = three-dimensional
TRM = treatment response mapping

Author contributions:
Guarantors of integrity of entire study, F.C.H., J.M.W.; study concepts/study design or data acquisition or data analysis/interpretation, all authors; manuscript drafting or manuscript revision for important intellectual content, all authors; manuscript final version approval, all authors; agrees to ensure any questions related to the work are appropriately resolved, all authors; literature research, F.C.H., H.M., G.J.C., J.M.W.; clinical studies, F.C.H., H.M., R.K., S.S., C.E.B., J.P., J.M.W.; experimental studies, F.C.H., H.M., G.J.C., J.P., J.M.W.; statistical analysis, F.C.H., J.P., J.M.W.; and manuscript editing, F.C.H., H.M., G.J.C., R.K., S.S., J.M.W.

Conflicts of interest are listed at the end of this article.

MR Imaging Data Acquisition

Prior to the imaging acquisition visit, participants refrained from using any short-acting bronchodilators for at least 6 hours. Patients were then imaged in a supine position with a clinical 1.5-T MR imaging unit (HDx; GE Healthcare, Milwaukee, Wis) with a dedicated MR ^{3}He RF coil. Hydrogen 1 MR imaging was performed with the system's body coil. Each image was acquired on inhalation of 1 L of gas from a Tedlar bag (350 mL hyperpolarized ^{3}He mixed with 650 mL N_2) from functional residual capacity. Prior to imaging, patients were trained in the breathing maneuver. Three ventilation MR imaging acquisitions were performed in separate breath holds; two at baseline within 5 minutes of each other, then an additional acquisition 20 minutes after bronchodilator administration to assess short-term airway responsiveness (19) (Fig 1). Each breath-hold acquisition consisted of *(a)* functional images (hyperpolarized ^{3}He ventilation; resolution, 3 × 3 × 10 mm; duration, 9 seconds) and *(b)* structural images (^{1}H anatomy; resolution, 3 × 6 × 10 mm; duration, 4 seconds). To switch between ^{3}He and ^{1}H MR imaging, the imaging unit required approximately 3–5 seconds, leading to a total breath-hold duration of less than 18 seconds in all cases. Because both functional and structural images are acquired back-to-back during a single breath hold, they are intrinsically coregistered (20).

Table 1

Overview of Demographics and Results of Pulmonary Function Tests in 20 Patients with Asthma

Characteristic	Value
Age (y)	51 ± 12
Female:male ratio	10:10
Height (m)	1.66 ± 0.07
Weight (kg)	82 ± 15
BMI (kg/m^2)	30 ± 5
GINA classification	4.10 ± 0.68
No. of pack-years	0.62 ± 1.91
RV (L)	2.78 ± 1.18
TLC (L)	6.23 ± 1.54
FEV_1 (percentage predicted)	71 ± 28 (27–122)
FVC (percentage predicted)	92 ± 22 (54–138)
FEV_1/FVC (percentage predicted)	75 ± 17 (31–83)

Note.—Unless otherwise specified, all data are means ± standard deviations, with ranges in parentheses. All measurements were obtained before application of the bronchodilator. Spirometry was performed with a rolling seal Vitalograph spirometer (Vitalograph, Buckingham, England) according to guidelines (17). BMI = body mass index, FVC = forced vital capacity, GINA = Global Initiative for Asthma (16), pack-years = lifetime tobacco exposure (1 pack-year was defined as 20 cigarettes a day for a year), RV = residual volume, TLC = total lung capacity. Predicted values were calculated by using equations (18).

Image Processing Algorithm for TRM

Structural proton images were first registered between the different time points, and the resulting transformation was applied to the same breath-hold ^{3}He ventilation images (21). This avoided the registration of the ^{3}He ventilation images being influenced by regional changes in gas distribution between acquisitions (Appendix E1 [online]). Then, images were segmented to extract the ventilated lung volume by using ScanIP (Simpleware, Exeter, England).

Regional ventilation was then calculated from the image intensity for each data set. Ventilation as regional gas distribution in the lung is quantified by conversion of image intensity to the volume fraction occupied by the inhaled tracer gas in each voxel. This requires knowledge of voxel volume (V_{voxel}) and inhaled gas volume (V_{bag}), as described by Tzeng et al (10):

$$R'(\mathrm{r}) = \frac{I(r)}{V_{voxel}} \cdot \frac{V_{bag}}{I_{tot}}, \qquad (1)$$

where $I(r)$ is the regional image intensity at position $r(x,y,z)$, I_{tot} is the integrated image intensity of all ventilated areas in the image, and $R'(r)$ is the resulting regional gas volume fraction in each voxel. For example, in the trachea directly after inhalation, the gas composition is usually the same as that inhaled from the bag, and hence $R' = 1$.

To compare $R'(r)$ between data sets, the differences in gas dilution of the tracer gas in the ventilated airspaces have to be taken into account.

Figure 1

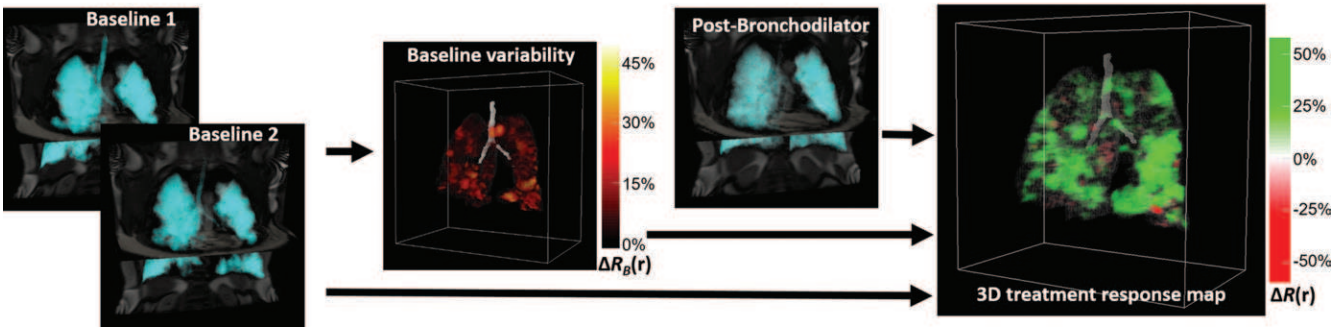

Figure 1: Image processing workflow from left to right: 3D image sets (proton and hyperpolarized gas ventilation image within a single breath hold) are acquired twice at baseline to calculate baseline variability. Twenty minutes after bronchodilator application, another 3D set is acquired. The differences between pre- and post-bronchodilator images are plotted as treatment response $\Delta R(r)$ maps and are compared with a regional treatment activation threshold from baseline variability, $\Delta R_B(r)$. This data set was obtained in a 54-year-old man (patient 2).

Table 2

Summary of Outcome Measures Used to Assess Treatment Response, Including ΔR_{net}

A: Absolute Measurements

Measurement	Before Bronchodilator	After Bronchodilator	*P* Value	Difference (before vs after Bronchodilator)	95% CI of Median	CV (%)*
FEV_1 (percentage predicted)	72 (44–96)	79 (58–100)	.0002	6.3 (4.5–13)	5.1, 12	99
FVC (percentage predicted)	85 (76–110)	93 (85–120)	.004	5.2 (1.9–8.3)	2.8, 8.0	137
FEV_1/FVC (%)	68 (48–73)	88 (65–91)	<.0001	3.6 (2.4–5.5)	2.7, 5.2	143
%VV at imaging	88 (83–94)	93 (90–97)	.0009†	3.5 (0.2–5.7)	0.41, 5.4	109

B: Differential Measurements

Outcome Metric	Positive ΔR_{net}	Negative ΔR_{net}	*P* Value	ΔR_{net}	95% CI	CV (%)
ΔR_{net} (%)	20 (16–26)	9 (7–11)	<.0001†	11 (6.6–14)	8.8, 12.4	64
ΔR_{net} (mL)	210 (160–260)	92 (71–110)	<.0001†	110 (66–140)	88.2, 123.9	64

Note.—All data are medians, with interquartile ranges (25th–75th quartile) in parentheses. Unless otherwise specified, *P* values were calculated with the paired *t* test. CI = confidence interval. Patient-specific values are shown in Tables E2 and E3 (online) alongside scatterplots in Figure E1 (online).

* CV = coefficient of variation (ratio of standard deviation to mean of treatment effect).

† Non–normally distributed data, so the Wilcoxon signed rank test was used.

After intervention, airway opening and closure will likely result in differences in ventilated lung volume. These variations can cause dilution of the tracer gas concentration when it is inhaled in the same dose from breath to breath. The ventilated lung volume after treatment (V_{LTx}) was chosen as the reference point, and the normalized gas volume fraction R was computed as follows:

$$R(\mathrm{r}) = R'(\mathrm{r}) \cdot \frac{V_L}{V_{LTx}}, \qquad (2)$$

where V_L is the ventilated lung volume calculated from the image of interest. Equation (2) assumes that regional gas concentration scales uniformly with lung volume changes across all voxels in the lungs.

The difference in gas volume fraction, $\Delta R(\mathrm{r})$, before and after intervention is then calculated for all positions (r) to quantify the treatment response map. $\Delta R(\mathrm{r})$ is, in effect, the regionally measured redistribution of the gas mixture when inhaling identical doses before and after intervention. Like $R(\mathrm{r})$, the treatment response map $\Delta R(\mathrm{r})$ is a gas volume fraction, which measures the size and direction of ventilation change due to intervention. The major airways were excluded, as they do not contribute to gas exchange and can be expected to be fully ventilated in each breath. To account for ventilation changes related to physiologic baseline variability from acquisition to acquisition, a voxelwise baseline variability map, $\Delta R_B(\mathrm{r})$, was calculated as the standard deviation of the differences in gas volume fraction $R(\mathrm{r})$ between the two (filtered) baseline acquisitions. $\Delta R(\mathrm{r})$ is set to zero (no effect) for voxels whose $/\ \Delta R(\mathrm{r})\ / \leq /\ \Delta R_B(\mathrm{r})\ /$ and is displayed as white voxels. For remaining voxels, a positive $\Delta R(\mathrm{r})$ (improvement in local ventilation) is shown with a green color scale, and a negative $\Delta R(\mathrm{r})$ (reduction in local ventilation) is shown with a red color scale. In addition, a global value for net treatment response over the whole lungs, ΔR_{net}, was calculated as follows:

$$\Delta R_{net} = \sum_{\mathrm{r}} \Delta R(\mathrm{r}) \cdot V_{voxel}. \qquad (3)$$

ΔR_{net} is summed over the lung volume and can be expressed as the percentage of the inhaled gas mix (1 L) or, alternatively, in milliliters, as the volume of the gas dose that is delivered to newly ventilated regions of the lung after inhalation of a 1-L dose. We emphasize that expression of ΔR_{net} in milliliters is not to be confused with the volume of the lungs that opens up in response to the bronchodilator; instead, it is the amount of the tracer gas (from a 1-L total inhaled dose), that reaches newly ventilated lungs. For an inhaled gas mix of 1 L, a theoretical redistribution of ΔR_{net} = 100% or +1 liter would therefore mean a complete redistribution of all inhaled gas in previously non- or little-ventilated regions. The metric quantifies the sum of regional gas redistribution as result of the same dose inhaled before and after an intervention.

Accordingly, the global positive and negative change can be calculated by taking only positive or negative $\Delta R(\mathrm{r})$ into account. An analysis of error propagation related to these steps of performing TRM is presented in Appendix E1 (online).

Percentage Ventilated Volume

Percentage ventilated volume was calculated as the ratio of lung ventilated volume (from segmented ^{3}He ventilation images) to the total volume of the lung in the thorax (from segmentation of the ^{1}H image), as described previously (20).

Spirometry

Spirometry was performed with a rolling seal spirometer (Vitalograph, Buckingham, England) before and 20 minutes after bronchodilator inhalation according to American Thoracic

Figure 2

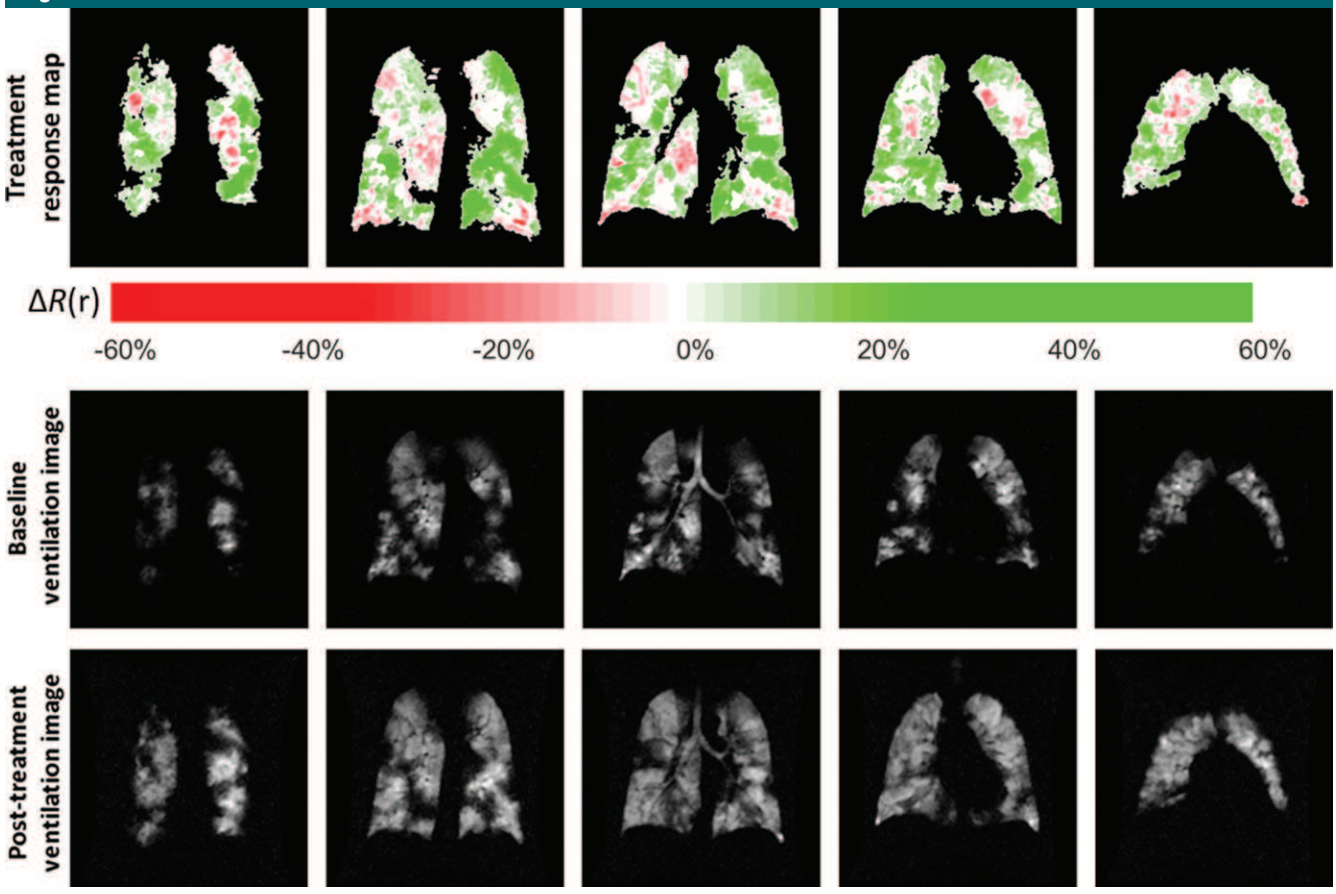

Figure 2: Examples of coronal treatment response maps (top row), MR ventilation images at baseline (middle row), and MR ventilation images after bronchodilator inhalation (bottom row). These images were obtained in patient 2, a 54-year-old man. The positive ΔR_{net} of 35.1% is compared with the negative ΔR_{net} of 5.5%, resulting in a total ΔR_{net} of +29.7%.

Society/European Respiratory Society guidelines (17). A minimum of three acceptable FVC maneuvers were performed, and the highest FEV_1 and FVC of the acceptable curves were recorded. Percentage predicted values were calculated as previously described (18). All pre-bronchodilator tests were performed after all bronchodilators had been withheld for at least 6 hours.

Statistical Analysis

Statistical analysis was performed by using Prism (GraphPad Software, San Diego, Calif). All data sets were first tested for normality by using a D'Agostino-Pearson omnibus normality test. Significance of treatment effect was tested by using a paired *t* test or, in the case of a nonnormal distribution, the Wilcoxon signed-rank test. The probability that the null hypothesis (H_0 = no treatment effect is found) can be rejected was tested (for $P < .05$ H_0 rejected). Values are reported as medians ± interquartile ranges (25th–75th quartiles). Correlations were calculated by using the Pearson *r* correlation (Spearman correlation in the case of nonnormality), and the correlation coefficient and *P* value of correlation are reported. $P < .05$ was considered to indicate a significant difference.

Results

An overview of results from the global MR imaging metrics (ΔR_{net}, %VV) and lung function test measurements (FEV_1, FVC) is presented in Table 2 (details for each patient are presented in Tables E2 and E3 [online]). TRM indicated an overall positive effect of the bronchodilator, in agreement with other metrics; the *P* values from paired *t* testing are shown in Table 2. An average intersubject baseline variability ΔR_B of 4.74% ± 4.68 was found. Example ^{3}He ventilation images and the resulting ΔR maps in patient 2 are shown in Figure 2. Three-dimensional renderings of treatment response maps in four more patients are shown in Figure 3. Figure 4 shows correlation of ΔR_{net} with changes in the other metrics evaluated: %VV ($r = 0.56$; $P = .01$), FEV_1 ($r = 0.70$; $P < .01$), and FVC ($r = 0.84$; $P < .01$). ΔR_{net} and FEV_1/FVC did not correlate significantly. The intersubject coefficient of variation of ΔR_{net} was 64%, which is much lower than those of %VV and spirometry (both ≥ 99%). Figure 5 shows the changes as assessed by all

Figure 3

Patient Number	Patient 5	Patient 8	Patient 10	Patient 11
(gender,age)	(male,41)	(male,59)	(female,62)	(female,45)
Baseline FEV_1(% pred.)	69.9	95.2	43.5	71.8
positive/negative ΔR_{net} [%]	27/7	20/9	33/10	28/7
ΔR_{net} volume [ml]/[%]	199/20	111/11	227/23	212/21

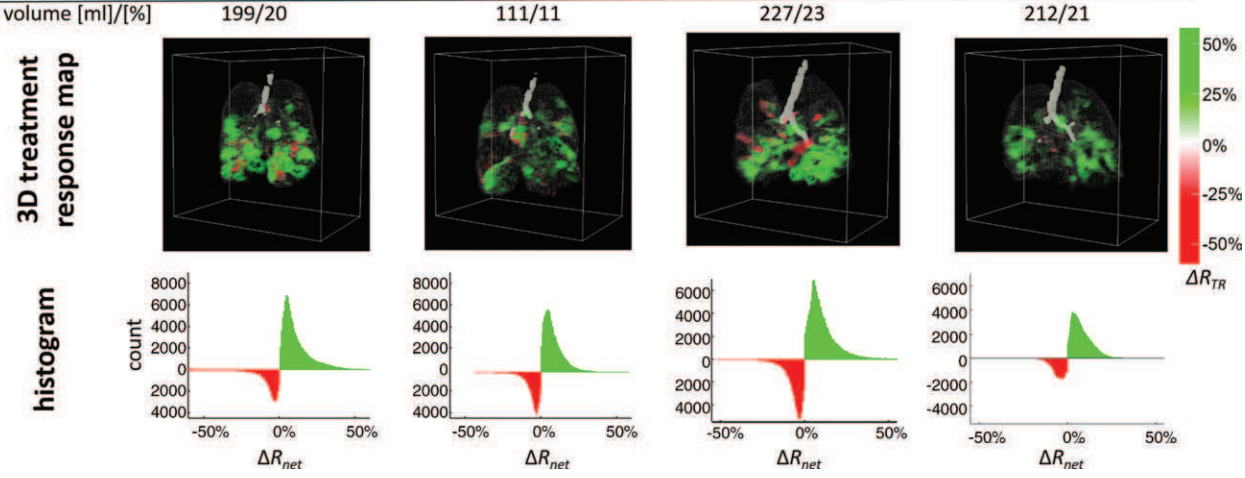

Figure 3: Example 3D-rendered treatment response maps in four volunteers, along with corresponding histograms.

Figure 4

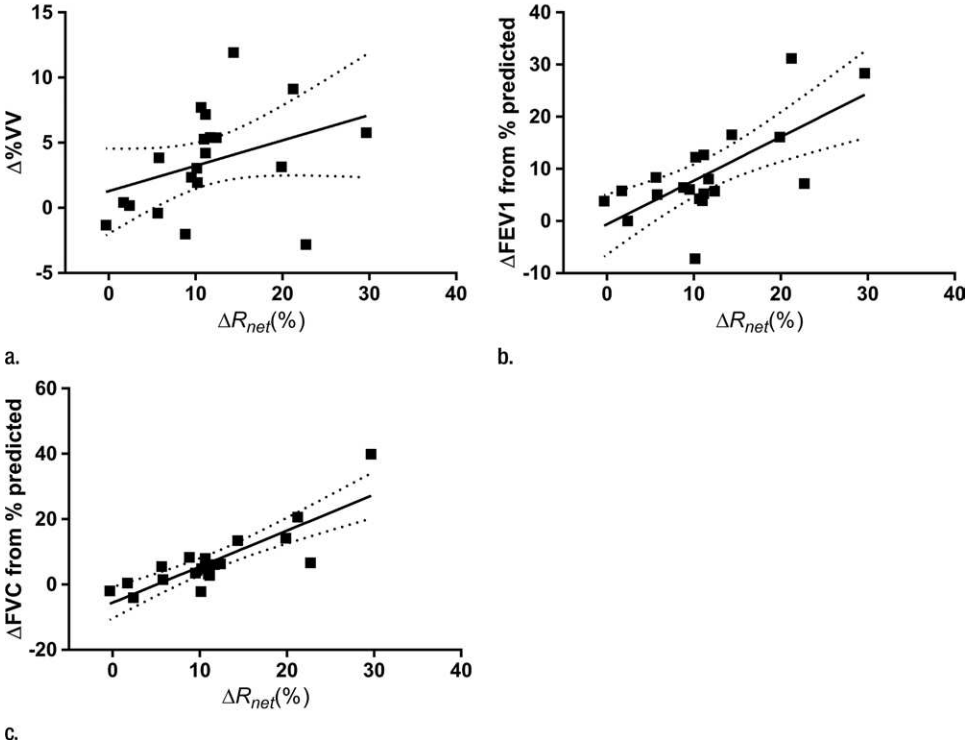

Figure 4: Graphs show **(a)** correlation of ΔR_{net} (as a percentage) with changes in %VV from before and after treatment (Δ%VV) (Spearman $r = 0.56$, $P = .01$), **(b)** correlation of ΔR_{net} with changes in FEV_1 from treatment (ΔFEV_1) (Pearson $r = 0.70$, $P = .004$), and **(c)** correlation of ΔR_{net} with FVC (Pearson $r = 0.84$, $P < .001$). Dotted lines = 95% confidence intervals.

Figure 5

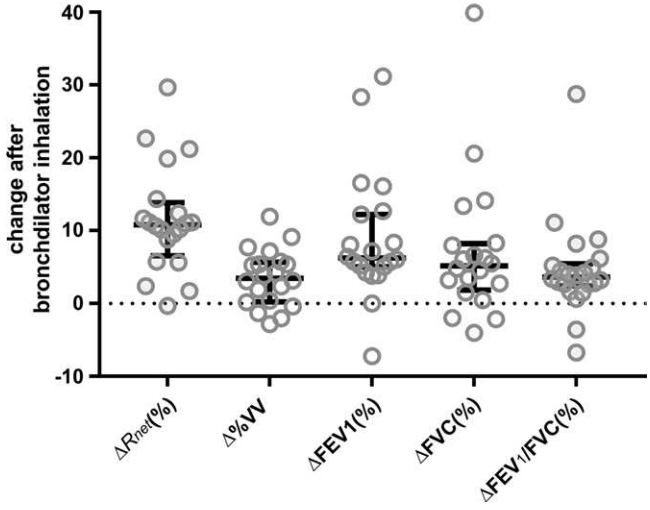

Figure 5: Graph shows comparison of changes from bronchodilator given the data in Table 2. Each plot shows median ± interquartile range interval, including each data point. Changes are expressed as differences in percentage predicted value (FEV_1/FVC, FVC, FEV_1), difference in %VV before and after treatment, and percentage ΔR_{net}. The plot shows that the treatment effect found from ΔR_{net} was greater on average and the standard deviation was smaller than those of the spirometric indexes.

methods for each patient and their collective median (interquartile range).

Discussion

TRM of changes in lung ventilation in response to therapy is demonstrated here with pre- and post-bronchodilator imaging in a cohort of patients with asthma. The effects of a bronchodilator are typically clinically assessed with spirometry, airway resistance, or static lung volume measurement. Although these methods are quick and easy to repeat, regional changes in lung ventilation and airway opening and closing are not accessible with these methods. This is likely to reduce the sensitivity of these clinical tests to subtle but still clinically important changes in ventilation, in particular when the treatment is focused on a small lung region (eg, with bronchothermoplasty or endobronchial valves). Imaging as a diagnostic tool can provide regional insight into alterations of both the structure and the function of the lung. Airway wall measurements and models of lobar ventilation change from inspiratory and expiratory computed tomography (CT) have both been proposed as image-based outcome measures in asthma (6), but the repeated exposure to ionizing radiation is an issue. Hyperpolarized gas MR imaging directly measures functional information from the lungs without ionizing radiation, and TRM is a potentially powerful tool for longitudinal and pediatric studies. Previously, oxygen-enhanced MR imaging has been used to measure changes induced by bronchodilators and corticosteroids (22). However, it is unclear to what extent this method captures changes in ventilation, as signal changes are caused by the interaction of protons with O_2 dissolved in tissue and blood (23).

Signal intensity from hyperpolarized gas MR images is proportional to the distribution of inhaled tracer gas in the lung and is therefore a direct measure of ventilation. The TRM method demonstrated here uses this relationship to regionally quantify the magnitude of ventilation changes.

The inherent baseline variability of the images from acquisition to acquisition without any intervention is also taken into account in the algorithm and defines a voxelwise threshold for "treatment response." This is important as it has been previously shown that originally nonventilated regions of the lung can change size and position on the same day in patients with asthma without intervention (13).

One of the most striking findings was the close correlation of FVC and FEV_1 with the global TRM metric ΔR_{net}. The fact that imaging and spirometry were not performed on the same day represents a limitation of this study and might explain why the correlations between spirometry and ΔR_{net} were not stronger. Although all of the tested metrics showed a significant effect from the bronchodilator ($P < .01$), the largest changes were found from ΔR_{net} (Fig 5). The intersubject coefficient of variation of ΔR_{net} was also smaller (64%) than for the other metrics (≥99%).

Some improvements in FVC were high (39% for patient 2) and might reflect recruitment of air spaces due to decreased gas trapping, an assumption that is supported by increases in %VV (5.8% for patient 2) in most patients. The weaker correlation ($r = 0.56$) of ΔR_{net} with changes in %VV supports the assumption that changes in ventilation are not only a result of a net increase in viable ventilated airspace volume but also reflect changes in heterogeneity of the magnitude of the ventilation that are regionally elucidated with the TRM method.

In patients with a limited spirometric response (<12%) to a bronchodilator, TRM effectively distinguishes regions of the lung with an increase in ventilation from regions demonstrating reduced ventilation. This lends some regional evidence to the possibility that bronchodilators are not always effective and can be potentially detrimental in selected regions of the lung in asthma. Similar observations have been reported in other imaging biomarker studies (22). Nevertheless, negative ΔR(r) can result from two other mechanisms; while a degradation of ventilation is

observed in practice in some lung regions after treatment, other regions of negative $\Delta R(r)$ might result from initially hyperventilated regions of lung that were perhaps compensating for obstruction elsewhere, then returning to more-even levels after bronchodilator application. Understanding the physiologic mechanism and phenotyping these "red regions" of worsened ventilation warrants further investigation.

In conclusion, TRM is able to complement the current techniques for regionally quantifying changes in ventilation in the lungs. The future clinical potential of the method lies in determining the regional response of the lungs to new therapies where established lung function tests do not provide sensitive enough outcome measures. This sensitivity to local changes in ventilation could also result in a reduction of patient cohort numbers required to confirm success of a treatment in a clinical trial.

Current limitations of the technique include the requirement for hyperpolarized gas MR imaging infrastructure for effective delivery in a clinical setting. Recent advances may help overcome this barrier in years to come, as the technique may also be directly applicable to ventilation images acquired by using other gases to image lung function, such as hyperpolarized ^{129}Xe or fluorine 19 fluorinated gases like perfluoropropane (24,25).

Acknowledgments: The authors acknowledge Professor David Barber and Bilal Tahir for their help with the image registration. The authors acknowledge research administrators Amisha Singapuri and Leanne Armstrong for their help in organizing the study.

Disclosures of Conflicts of Interest: F.C.H. disclosed no relevant relationships. **H.M.** disclosed no relevant relationships. **G.J.C.** disclosed no relevant relationships. **R.K.** Activities related to the present article: is an employee of Novartis Pharmaceuticals. Activities not related to the present article: disclosed no relevant relationships. Other relationships: disclosed no relevant relationships. **S.S.** disclosed no relevant relationships. **C.E.B.** disclosed no relevant relationships. **J.P.** disclosed no relevant relationships. **J.M.W.** disclosed no relevant relationships.

References

1. Hunter CJ, Brightling CE, Woltmann G, Wardlaw AJ, Pavord ID. A comparison of the validity of different diagnostic tests in adults with asthma. Chest 2002;121(4):1051–1057.
2. Vos W, Hajian B, De Backer J, et al. Functional respiratory imaging to assess the interaction between systemic roflumilast and inhaled ICS/LABA/LAMA. Int J Chron Obstruct Pulmon Dis 2016;11:263–271.
3. Dombret MC, Alagha K, Boulet LP, et al. Bronchial thermoplasty: a new therapeutic option for the treatment of severe, uncontrolled asthma in adults. Eur Respir Rev 2014;23 (134):510–518.
4. Gesierich W, Samitas K, Reichenberger F, Behr J. Collapse phenomenon during Chartis collateral ventilation assessment. Eur Respir J 2016;47(6):1657–1667.
5. Davey C, Zoumot Z, Jordan S, et al. Bronchoscopic lung volume reduction with endobronchial valves for patients with heterogeneous emphysema and intact interlobar fissures (the BeLieVeR-HIFi trial): study design and rationale. Thorax 2015;70(3):288–290.
6. De Backer JW, Vos WG, Devolder A, et al. Computational fluid dynamics can detect changes in airway resistance in asthmatics after acute bronchodilation. J Biomech 2008;41 (1):106–113.
7. Altes TA, Powers PL, Knight-Scott J, et al. Hyperpolarized 3He MR lung ventilation imaging in asthmatics: preliminary findings. J Magn Reson Imaging 2001;13(3):378–384.
8. Aysola R, de Lange EE, Castro M, Altes TA. Demonstration of the heterogeneous distribution of asthma in the lungs using CT and hyperpolarized helium-3 MRI. J Magn Reson Imaging 2010;32(6):1379–1387.
9. Tustison NJ, Altes TA, Song G, de Lange EE, Mugler JP 3rd, Gee JC. Feature analysis of hyperpolarized helium-3 pulmonary MRI: a study of asthmatics versus nonasthmatics. Magn Reson Med 2010;63(6):1448–1455.
10. Tzeng YS, Lutchen K, Albert M. The difference in ventilation heterogeneity between asthmatic and healthy subjects quantified using hyperpolarized 3He MRI. J Appl Physiol (1985) 2009;106(3):813–822.
11. He M, Driehuys B, Que LG, Huang YT. Using hyperpolarized (129)Xe MRI to quantify the pulmonary ventilation distribution. Acad Radiol 2016;23(12):1521–1531.
12. Kirby M, Heydarian M, Svenningsen S, et al. Hyperpolarized 3He magnetic resonance functional imaging semiautomated segmentation. Acad Radiol 2012;19(2):141–152.
13. de Lange EE, Altes TA, Patrie JT, et al. Changes in regional airflow obstruction over time in the lungs of patients with asthma: evaluation with 3He MR imaging. Radiology 2009;250(2):567–575.
14. de Lange EE, Altes TA, Patrie JT, et al. Evaluation of asthma with hyperpolarized helium-3 MRI: correlation with clinical severity and spirometry. Chest 2006;130(4):1055–1062.
15. Kirby M, Svenningsen S, Owrangi A, et al. Hyperpolarized 3He and 129Xe MR imaging in healthy volunteers and patients with chronic obstructive pulmonary disease. Radiology 2012;265(2):600–610.
16. Busse WW, Boushey HA, Camargo CA, et al. Guidelines for the Diagnosis and Management of Asthma 2007. http://www.nhlbi.nih.gov/files/docs/guidelines/asthsumm.pdf. Accessed July 29, 2014.
17. Miller MR, Hankinson J, Brusasco V, et al. Standardisation of spirometry. Eur Respir J 2005;26(2):319–338.
18. Quanjer PH, Stanojevic S, Cole TJ, et al. Multi-ethnic reference values for spirometry for the 3-95-yr age range: the global lung function 2012 equations. Eur Respir J 2012;40(6): 1324–1343.
19. James DR, Lyttle MD. British guideline on the management of asthma: SIGN Clinical Guideline 141, 2014. Arch Dis Child Educ Pract Ed 2016;101(6):319–322.
20. Horn FC, Tahir BA, Stewart NJ, et al. Lung ventilation volumetry with same-breath acquisition of hyperpolarized gas and proton MRI. NMR Biomed 2014;27(12):1461–1467.
21. Barber DC, Oubel E, Frangi AF, Hose DR. Efficient computational fluid dynamics mesh generation by image registration. Med Image Anal 2007;11(6):648–662.
22. Morgan AR, Parker GJ, Roberts C, et al. Feasibility assessment of using oxygen-enhanced magnetic resonance imaging for evaluating the effect of pharmacological treatment in COPD. Eur J Radiol 2014;83(11):2093–2101.
23. Mills GH, Wild JM, Eberle B, Van Beek EJ. Functional magnetic resonance imaging of the lung. Br J Anaesth 2003;91(1):16–30.
24. Halaweish AF, Moon RE, Foster WM, et al. Perfluoropropane gas as a magnetic resonance lung imaging contrast agent in humans. Chest 2013;144(4):1300–1310.
25. Stewart NJ, Norquay G, Griffiths PD, Wild JM. Feasibility of human lung ventilation imaging using highly polarized naturally abundant xenon and optimized three-dimensional steady-state free precession. Magn Reson Med 2015;74(2):346–352.